SIGNAL PROCESSING

Signal Processing 54 (1996) 295–301

# Sodar image segmentation by fuzzy *c*-means

D.P. Mukherjee*, P. Pal, J. Das

*Electronics and Communication Sciences Unit, Indian Statistical Institute, Calcutta 700 035, India*

Received 25 September 1995; revised 15 January 1996 and 6 May 1996

**Abstract**

Sodar facsimile records provide meteorological information of the atmospheric boundary layer (ABL). Segmentation of sodar image (digitised sodar record) is vital for subsequent interpretation of ABL structure. The problem of segmentation is presented here as classification problem. Fuzzy *c*-means classification algorithm has been adopted for segmentation purpose using a set of four feature vectors calculated over a mask such that they characterise the nature of local grey value distribution. The classified images are also compared to another segmentation technique. The results presented prove the definite merits of the proposed technique.

**Zusammenfassung**

Faksimile-registrierungen von SODAR liefern meteorologische Information über die atmosphärische Grenzschicht (ABL). Die Segmentierung des SODAR Bildes (also der digitalisierten SODAR Registrierung) ist entscheidend für die darauffolgende Interpretation der ABL Struktur. Das segmentierungsproblem wird hier als Klassifikationsproblem behandelt. Der fuzzy *c*-means Klassifikationsalgorithmus wurde für die Segmentierungsaufgabe angepaßt, wobei ein Satz von vier Merkmalsvektoren zum Einsatz kommt, die derart über eine Maske berechnet werden, daß sie die Natur der lokalen Grauwertverteilung charakterisieren. Die klassifizierten Bilder werden auch mit einem anderen Segmentierungsverfahren verglichen. Die vorgestellten Ergebnisse zeigen die eindeutigen vorzüge des vorgeschlagenen Verfahrens auf.

**Résumé**

Les enregistrements facsimilé de sodars fournissent des informations météorologiques sur la couche frontière de l'atmosphère (CFA). La segmentation d'images sodar (enregistrement de sodar numerisé) est vitale pour l'interprétation subséquente de la structure de la CFA. Le problème de segmentation présenté ici est un problème de classification. Un algorithme de classification '*c*-means' flou a été adopté pour cette segmentation, utilisant un ensemble de 4 vecteurs de caractéristiques, calculés sur un masque défini de telle sorte qu'ils caractérisent la nature de la distribution locale des valeurs de gris. Les images ainsi classées sont également comparées à une autre technique de segmentation. Les résultats présentés ici prouvent les mérites manifestes de la technique proposée.

*Keywords*: Sodar; Atmospheric boundary layer (ABL); Segmentation; Classification; Fuzzy *c*-means

## 1. Introduction

SODAR (SOnic Detection And Ranging) facsimile record generates valuable meteorological information of ABL (Atmospheric Boundary Layer) within 1 km height vertically upwards from the Earth's surface. Meteorologist can qualitatively predict some form of weather conditions by looking at the shapes (such as plumes, inversion, multilayered, etc.) generated in the sodar recorder. This prediction is based on the shape of the signal and not on the overall signal quality. The detection of the sodar signal pattern, therefore, should be the frontend of any automated sodar data interpretation system for generating a human-like weather prediction system. This, however, needs separation of pixels representing sodar signal and pixels representing background due to white portion of the facsimile page. In this paper, the sodar facsimile record is scanned and the resultant 2D digitised image is subjected to such segmentation using fuzzy $c$-means approach. Two typical examples of sodar images are shown in Figs. 1(a) and (b).

Unfortunately, the backscattered sodar signal contains other environmental and atmospheric noises such as noises due to horn of an automobile, chirping of a bird or even rain noises. Therefore, the algorithm, presented in this paper, segments pixels representing sodar information from the combined pixel class representing noise and background. Methodology of segmentation is presented, and then followed by the result and discussion.

## 2. Methodology

Different methodologies [7, 2] have been developed for segmenting sodar images. In [7], the threshold value has been manually selected by observing the grey level histogram and the grey value corresponding to the point in the valley (of the histogram) from where the slope rises sharply is selected as threshold point. A nonparametric and unsupervised method of automatic threshold selection proposed by Otsu [6] has been used in [2]. Based on local grey value distribution, Mukherjee et al. [5] have developed a masking technique which when added to the horizontal components of edge detecting Sobel [3] mask, generates *almost* segmented image in case of sodar image.

In this paper, fuzzy-$c$-means classification algorithm [1] is used to segment the sodar image into pixel clusters representing signal and background. From the typical sodar images, it is clear that the separation of different clusters are not *well-defined*, rather *fuzzy*, and depends on the local grey value distribution. Because of noises (as stated in the introduction), additional fuzziness is introduced in the pixel value while selecting it to be a member of either signal

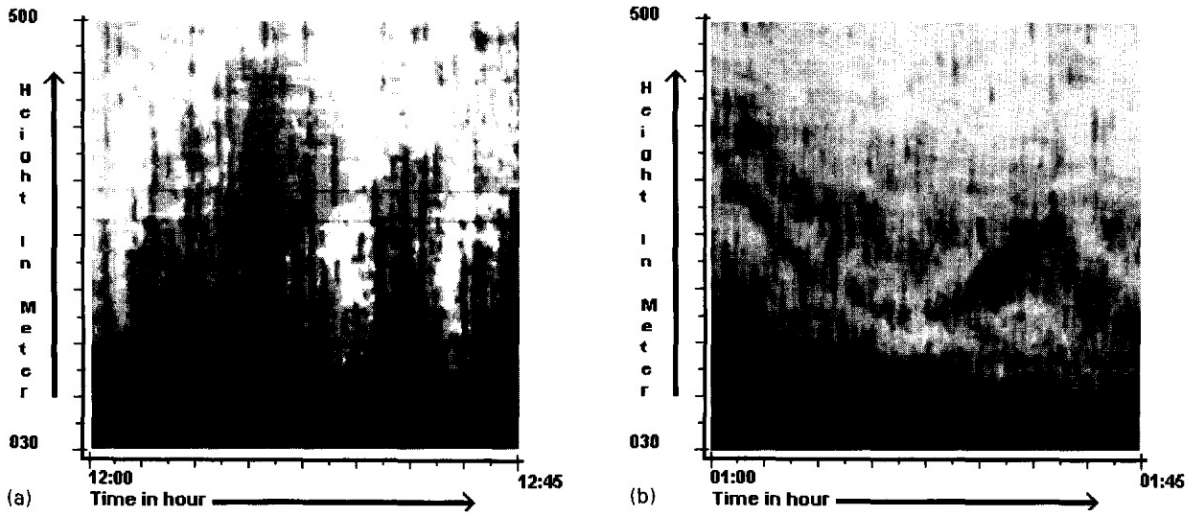


Fig. 1. Sodar images: (a) plume structure; (b) multilayered structure.

class or noise and background class, clubbed together. Keeping in mind these characteristics, we have selected a set of feature vectors which are strictly local in nature, that is, depends on 8-neighbourhood of the pixel concerned. Since, fuzzy $c$-means technique provides an iterative measure to minimize the classification error allowing each pixel to be the member of all the possible classes with varying membership, it seems appropriate to apply this algorithm. In the next section we present fuzzy-$c$-means fundamentals followed by the details of the feature vectors.

## 3. Fuzzy-$c$-means fundamentals

The clustering algorithm is based on a least-squared error criterion

$$J_m(U, v) = \sum_{k=1}^{n} \sum_{i=1}^{c} (u_{ik})^m (d_{ik})^2,$$

where $U$ is a fuzzy $c$-partition of data set $X$, a matrix containing feature vector values for each pixel. Vector $u_{ik}$ contains the fuzzy membership value of $k$th data point (pixel) to $i$th class. The vector $v_i$, whose number of components depends on the number of feature vectors, is the cluster center of $i$th class of fuzzy $c$-partitions, also called seed point for the particular class. These are updated in every iteration based on $u_{ik}$ and the distance $d_{ik} = ||X_k - v_i||$, between $i$th cluster center of $v$ and $k$th data point of $X$. This continues till the cluster centers become stable and there is *insignificant* difference between cluster centers in two consecutive iterations. The weighting exponent is $m$ where $m \in [1, \infty)$.

To *minimize* $J_m(U, v)$ subject to the condition $\sum_{i=1}^{c} u_{ik} = 1$, $0 < \sum_k u_{ik} < k$ and $u_{ik} \geqslant 0$, applying Lagrange multipliers to the variables $u_{ik}$, we obtain

$$u_{ik} = 1 \Big/ \left[ \sum_{j=1}^{c} \left( \frac{d_{ik}}{d_{jk}} \right)^{2/(m-1)} \right] \tag{1}$$

and $\forall i$

$$v_i = \frac{\sum_{k=1}^{n} (u_{ik})^m X_k}{\sum_{k=1}^{n} (u_{ik})^m}. \tag{2}$$

In every iteration, $u_{ik}$ is calculated using Eq. (1) while $v_i$ is updated following Eq. (2) using the earlier $u_{ik}$ value. In every iteration, the condition $\sum_{i=1}^{c} u_{ik} = 1$ is ensured while, initially, $u_{ik}$ is generated using random number function. The algorithm is terminated for *insignificant* (1–2% of the current value) changes between two consecutive $v_i$ values. From the implementational standpoint, the algorithm has two modules.

*Training module.* The fuzzy $c$-means clustering algorithm is applied to a chunk of the original image. The images with all the clusters present in significant proportions are chosen. We find that the cluster seed points stabilizes after 10–12 iterations. The output of $v_{in}$ gives seed point for $i$th class and $n$th feature vector for further classification while the $u_{ik}$ gives the fuzzy membership value of the $k$th data point associated with the $i$th class. The cluster centers of different feature vectors are matched with corresponding pixel classes by visual inspection.

*Classification module.* To reduce processing time in case of large image, the pixels are classified based on their highest membership values in $u_{ik}$ associated with the particular class. Also the pixels could be classified based on the minimum distance $d_{ik}$ between the feature vectors for the pixel and the seed points of the classes.

### 3.1. Feature vectors

Since, we have no a priori information about the cluster seed points, image texture or grey value distribution, we have selected feature vectors such that they represent the closest possible nature or homogeneity of any image subregion. Using standard masking techniques of image processing, for the subimage,

| | | |
|---|---|---|
| $m_{00}$ | $m_{01}$ | $m_{02}$ |
| $m_{10}$ | $m_{11}$ | $m_{12}$ |
| $m_{20}$ | $m_{21}$ | $m_{22}$ |

the following feature vectors are calculated for $m_{11}$:

1. The average grey values ($A$) of $m_{11}$, $A(m_{11}) = \frac{1}{9} \sum_{i=0,j=0}^{2,2} m_{ij}$.
2. The busyness value ($B$) of $m_{11}$, $B(m_{11}) = \min(B_h, B_v)$, where $B_h = \sum_{i=0}^{2} |m_{i0} - m_{i1}| + |m_{i1} - m_{i2}|$ and $B_v = \sum_{j=0}^{2} |m_{0j} - m_{1j}| + |m_{1j} - m_{2j}|$.

The busyness value is influenced by the (horizontal or vertical) orientation of grey value distribution.

3. The absolute difference between the maximum and minimum grey value of the subimage, a local measure of contrast, $(D)$ of $m_{11}$, $D(m_{11}) = |\max(m_{ij}) - \min(m_{ij})|$, where $i = [0,2]$ and $j = [0,2]$.
4. Entropy value [4] of $m_{11}$. Borrowing the classical definition of entropy based on the mathematical expectation of the information concerning the occurrence of one of the events, the entropy $E_i$ is given by $E(p_1, p_2, ..., p_n) = -\sum_1^n p_i \log p_i$, where $p_i > i$, $\sum_{i=1}^p p_i = 1$. Extending this in case of 2D image matrix with certain grey value distribution, $E(m_{11}) = \sum_{i=0,j=0}^{2,2} P_{ij} \log_{10} P_{ij}$, where $P_{ij} = m_{ij} / \sum_{i=0,j=0}^{2,2} m_{ij}$.

## 4. Results

Figs. 2(a) and (b) are the segmented images of plume structure (Fig. 1(a)) and multilayered structure (Fig. 1(b)), respectively, classified into two classes. Note that the images are not preprocessed with any filtering algorithm like neighbourhood or median filtering; still the segmentation is *clear* with minimum isolated small patches of pixels. In both the cases, the desired plume shape and the multilayered structure are clearly extracted using classification.

Since, it is expected that the plume structure will be having an envelope with signals of lower amplitude (which corresponds to lower grey value in the image), the image in Fig. 1(a) is subjected to classification algorithm with three classes. The result clearly supports the expected outcome as shown in Fig. 3. Here an envelope is formed at the upper portion of the plume, separating the core of the plume from its contour. This happens because the total energy confined at the center is being dissipated at its contour due to atmospheric condition. This may help in finding the region of energy dissipation of the plume. Also, the stray pixel columns indicate the direction of energy dissipation.

Fig. 4(b), a (two-class) classified plume structure image of Fig. 4(a), demonstrates the potential of our proposed approach. The seed vector used in this case is the one generated from the training module while classifying the plume image of Fig. 2(a). Therefore, in classifying Fig. 4(a), only classification and no training is performed using *instant* seed point, developed earlier for plume structure. This results in tremendous saving of cpu time and turns the cpu-intensive fuzzy $c$-means almost real time. Similar experiments are performed for other plume and multilayered structures and it could be confirmed that for *almost* similar weather conditions, *ready-to-use* seed point vectors, evaluated using fuzzy $c$-means could be used for instant classification of sodar images.

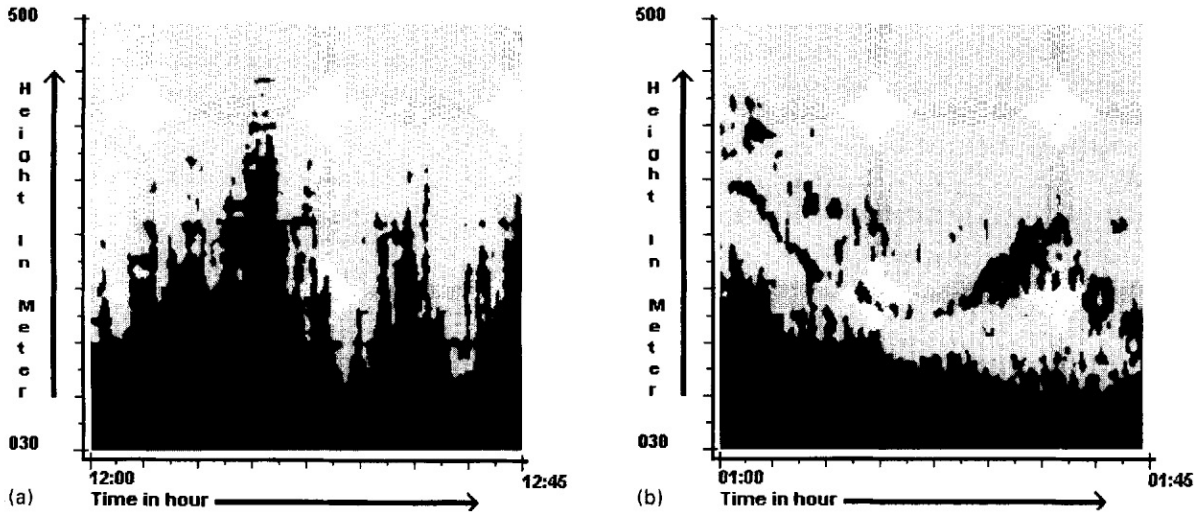


Fig. 2. (a) Plume structure of Fig. 1(a); (b) multilayered structure of Fig. 1(b) are classified into two classes.

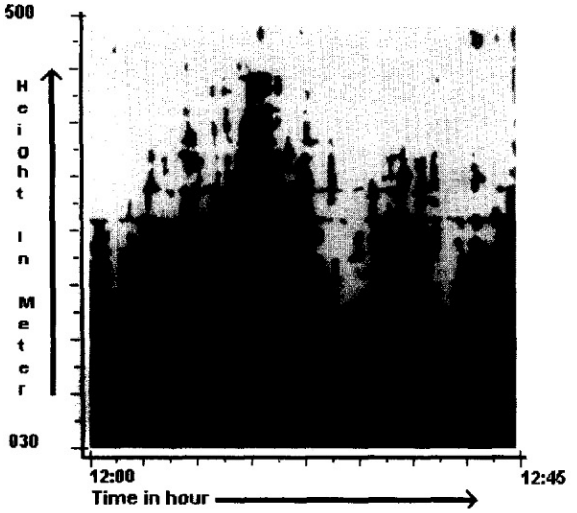


Fig. 3. The plume structure of Fig. 2(a) is classified into three classes. The energy fading at the plume envelope is detected as a separate class.

### 4.1. Comparison with another method

We have observed that segmentation of sodar images using Otsu's [6] thresholding criterion gives satisfactory result [2] after image preprocessing, that is, image noise cleaning using either average, median or max-min filtering. This approach is based on the evaluation of a measure of *goodness* of threshold and is detailed in [6].

Figs. 5(a) and (b) are the bilevel thresholded images (thresholded at 206 and 204) of Figs. 1(a) and (b), respectively, using Otsu's [2] thresholding criterion. Readers can compare this result with the segmentation obtained by fuzzy $c$-means classification as shown in Figs. 2(a) and (b), respectively.

Fig. 6 is given to compare the result of multilevel thresholding (three classes) with that of Fig. 3. Subjectively, the results using Otsu's method is comparable to that of fuzzy classification approach. However, Figs. 5(a) and (b) or Fig. 6 contain more number of isolated pixel patches, position and size of which clearly indicate that those are noise patches misclassified as information cluster.

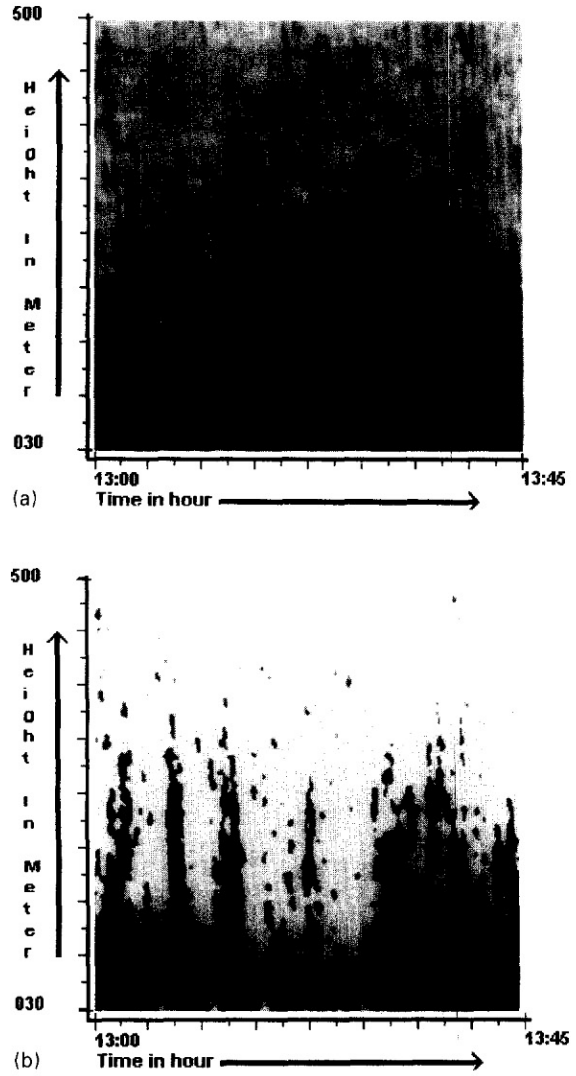


Fig. 4. (a) A plume structure. (b) The classification of (a) into two classes using seed point vectors of the information and background classes of Fig. 2(a).

Table 1 presents the classwise statistics of different classes for all the figures presented so far. The table clearly shows that the percentage of pixels grouped into clusters (for comparable images) are *almost* identical. The global class mean of grey value for classified images, considering all the pixels grouped into a single cluster, are comparable though their standard deviations, in case of fuzzy $c$-means, are higher compared to that of Otsu's method. Even though fuzzy $c$-means approach allows for higher class variance,

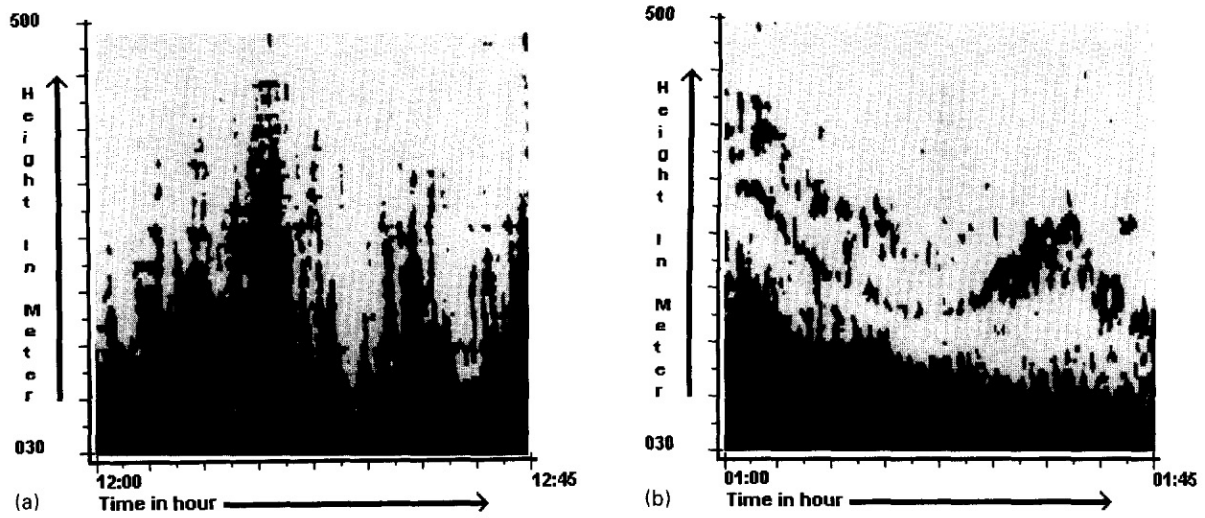


Fig. 5. (a) The plume structure of Fig. 1(a) is thresholded at grey value 206. (b) The multilayered structure of Fig. 1(b) is thresholded at grey value 204 using Otsu's [6] method.

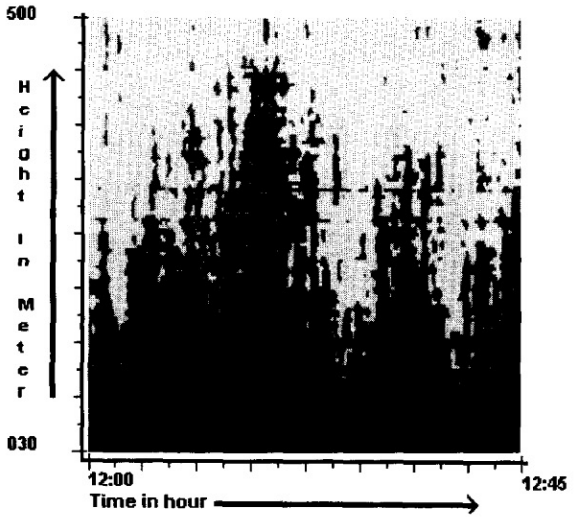


Fig. 6. The plume structure of Fig. 1(a) is segmented into three classes using Otsu's [6] method.

in this case, the feature vectors, particularly average and busyness parameters have increasing influence on the higher variance value. However, this possibly reduces the small isolated patches of pixels compared to the results obtained in case of thresholding method.

## 5. Discussion

We have shown that fuzzy-*c*-means-based segmentation technique has provided stable and attractive result even avoiding the expensive pixel by pixel noise filtering. However, the bottleneck is the *significant* processing time of the order of 5 min in SUNSPARC 10 while performing the *training* considering four feature vectors and three classes. This could be implemented in *almost* real time using parallel hardware as subblocks of image could be processed almost independently. However, possibility of using *ready-to-use* specific seed point vector (refer Fig. 4(b) which is classified using cluster seed vectors of Fig. 2(a)) under similar weather conditions could make this segmentation almost instantaneous.

## Acknowledgements

This work is partially supported by DST, Government of India. We would also like to thank Indranil Dutta for printing the images.

Table 1
Classwise statistics of results using fuzzy $c$-means and Otsu's method

| | Class 1 | | | Class 2 | | | Class 3 | | |
|---|---|---|---|---|---|---|---|---|---|
| Figure | % | Mean | Variance | % | Mean | Variance | % | Mean | Variance |
| 2(a) (F) | 43.96 | 181 | 796 | 56.04 | 228 | 639 | | | |
| 5(a) (O) | 44.45 | 170 | 273 | 55.55 | 235 | 191 | | | |
| 2(b) (F) | 32.52 | 191 | 1004 | 67.48 | 229 | 562 | | | |
| 5(b) (O) | 32.9 | 174 | 266 | 67.1 | 236 | 166 | | | |
| 3 (F) | 34.75 | 176 | 652 | 40.55 | 233 | 410 | 24.7 | 208 | 965 |
| 6 (O) | 34.43 | 163 | 118 | 42.38 | 242 | 67 | 23.19 | 206 | 131 |

Note: F denotes fuzzy $c$-means results whereas O denotes Otsu's method.

## References


[1] J.C. Bezdek, *Pattern Recognition with Fuzzy Objective Function Algorithms*, Plenum Press, New York, 1981.

[2] A.K. De, D.P. Mukherjee, P. Pal and J. Das, "Sodapreter: A novel approach towards automatic sodar data interpretation", *Internat. J. Remote Sensing*, Communicated.

[3] R.C. Gonzalez and P. Wintz, *Digital Image Processing*, Addison-Wesley, Reading, MA, 1987.

[4] Z.Q. Gu, C.N. Duncan, P.M. Grant, C.F.N.C.E. Renshaw and M.A. Mugglestone, "Textural and spectral features as an aid to cloud classification", *Internat. J. Remote Sensing*, Vol. 12, No. 5, 1991, pp. 953–968.

[5] D.P. Mukherjee, S.K. Tripathy, A. Chanda, A.K. De, P. Pal and J. Das, Mask design for enhancement of atmospheric images, An intermediate draft, 1995.

[6] N. Otsu, "A threshold selection method from grey level histograms", *IEEE Trans. Systems Man Cybernet.*, Vol. 9, 1979, pp. 61–65.

[7] S. Tripathi, A.K. De and J. Das, "Computer algorithm of noise removal in acoustic radar echograms", *Indian J. of Radio and Space Phys.*, Vol. 22, 1993, pp. 301–305.